

Use of 1.32- μm and 1.06- μm wavelength lasers for vascular cutting in a porcine model of liver and stomach bleeding*

Lu Han^{1, 2}, Wenyuan Gao (Co-first author)³, Yangyang Shen⁴, Kai Pang⁵, Zhanjun Jiang⁶, Yonghui Gao⁶, Peng Xu⁶ (✉), Sheng Li⁷ (✉)

¹ School of Medicine and Life Sciences, University of Jinan-Shandong Academy of Medical Sciences, Jinan 250062, China

² Department of Hepatobiliary Surgery, Shandong Academy of Medical Sciences, Shandong Cancer Hospital Affiliated to Shandong University, Jinan 250117, China

³ Shandong Academy of Medical Sciences, Shandong Cancer Hospital Affiliated to Shandong University, Jinan 250117, China

⁴ College of Medicine, Binzhou Medical University, Yantai 264003, China

⁵ Department of Anesthesiology, Shandong Academy of Medical Sciences, Shandong Cancer Hospital Affiliated to Shandong University, Jinan 250117, China

⁶ Optoelectronics Technology Co., Ltd. Shandong Ruihua TONGHUI, Jinan 250022, China

⁷ Shandong Academy of Medical Sciences, Jinan 250062, China

Abstract

Objective The aim of this study was to analyze and evaluate 1.32- μm and 1.06- μm neodymium-doped yttrium aluminum garnet (Nd:YAG) lasers for use in liver and gastroepiploic vessel vaporization and coagulation.

Methods The effects of 1.32- μm and 1.06- μm Nd:YAG lasers were compared for gastroepiploic vessel hemostasis in porcine liver.

Results The results were observed and measured under the same parameters and dose conditions. The 1.32- μm laser showed greater vaporization width and depth than the 1.06- μm laser. Both lasers controlled active bleeding. The coagulation band with the 1.32- μm laser was thinner than with the 1.06- μm laser, at nearly 3 mm. After cutting of 1- and 2-mm porcine vessels, no grossly visible bleeding was apparent. Intravascular thrombus was visible under the microscope. The length of vessel thrombosis in the experimental group was 2 mm and the diameter was 2 mm; the control group exhibited thrombi as 2.3–4.9 mm in length. Thrombosis completely blocked the blood vessels.

Conclusion The 1.32- μm laser had greater vaporization capability than the 1.06- μm laser and achieved hemostasis requirements for vessels less than 2 mm in diameter.

key words: laser; liver; stomach; cutting; hemostasis

Received: 5 December 2016

Revised: 11 February 2017

Accepted: 23 March 2017

The biological effect is an important aspect of laser use in medicine. Tissues absorb laser energy with irreversible damage to achieve treatment effects, such as coagulation, vaporization, cutting, and control of bleeding. Biological effects of lasers depend on wavelength, mode, power,

and other parameters. However, most studies have used a single-wavelength laser^[1–3]. Lasers have been studied in clinical surgery, but only for specific uses, such as coagulation, vaporization, cutting, and control of bleeding^[4–6]. With advances in technology, the indications for laser

✉ Corresponding to: Peng Xu. Email: syyvly@163.com
Sheng Li. Email: drlisheng@sohu.com

* Supported by a grant from the Medical Science and Technology Innovation Project of Shandong Academy of Medical Sciences.

© 2017 Huazhong University of Science and Technology

treatment have expanded. However, single-wavelength lasers cannot meet the needs of minimally invasive surgery.

Although lasers have been successfully used in clinical applications, there is a need for improvement in predictability, safety, and reliability. Bille and Niemz [7] described the interaction between laser theory and application in biological tissues. They reviewed the light-heat effect and thermal damage in organs. McKenzie [8] reviewed the physical process of laser-tissue interaction and discussed the use of heat conduction equations, various thermal effects produced by CO₂ and neodymium-doped yttrium aluminum garnet (Nd:YAG) lasers, angioplasty, hyperthermic therapy, and soft tissue welding. Diaz *et al* [9] used the finite element method to predict the thermal response to laser irradiation in porcine cartilage. By comparing surface and internal temperature measurements with theoretical results, they examined the impact of laser parameters and convective thermal response simulation on evaporated tissue. Kim *et al* [10] used nonlinear finite element methods to evaluate the effects of the Nd:YAG laser on dynamic changes in blood perfusion rates and optical parameters in coagulation of the canine prostate.

This research improved the understanding of the light-heat model. However, the experiments used limited temperature measurements and were performed *in vitro*. The use of living tissue with real-time temperature measurements encountered significant technical difficulty. Use of the equation model is limited in complex microvascular tissue because of difficulty in collecting the data.

The 1.06- μm Nd:YAG laser is the most commonly used in clinical applications [11–13]. The 1.32- μm laser is used less often. Biological tissue experiments [14] showed that 1.32- μm laser light is absorbed 10-fold more than 1.06- μm laser light, with deeper tissue penetration and better coagulation, hemostasis, and cutting efficiency, with less thermal damage. This study compared 1.32- μm and 1.06- μm laser irradiation in porcine liver for vaporization and coagulation efficacy. Different lasers were also compared with the 1.32- μm Nd:YAG laser for their efficacy in coagulation of porcine vessels for hemostasis.

Materials and methods

We used five male miniature pigs with average weight 37.82 kg. The equipment setup for a self-designed dual-wavelength (1.32 μm and 1.06 μm) laser surgery platform was shown in Fig. 1. Tissue was examined with an optical digital-scanning microscope (ZEISS Axioskop 40, Carl Zeiss Jena, Germany). Medical Image Analysis (Beijing Modern Fubo Technology Co., Ltd., China) and Management System

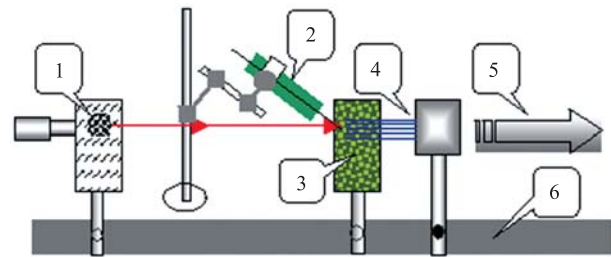


Fig. 1 A dual wavelength laser surgery platform (autonomous design). 1: Laser knife head bracket; 2: infrared radiation thermometer; 3: biological tissue; 4: microscope; 5: transmission laser beam; 6: experimental fixed platform

Table 1 selection and grouping of experimental parameters

| Group | Power (W) | Time (s) | Number |
|---|-----------|----------|----------------|
| Experimental group (1.32- μm) | 50 | 1 | G ₁ |
| | | 5 | G ₂ |
| | | 10 | G ₃ |
| Control group (1.06- μm) | 50 | 1 | G ₁ |
| | | 5 | G ₂ |
| | | 10 | G ₃ |

4.0 software was used for true color pathological image evaluation. SPSS 17.0 software (International Business Machines Corporation, America) was used for data analysis with a *t*-test.

The experimental group received 1.32- μm irradiation and controls received 1.06- μm irradiation. Two sets of laser output parameters were determined with 50 W power and time lapse of 1, 5, and 10 s. Fiber diameter was 800 μm (Table 1). Experiments were repeated five times.

Anesthesia was induced with 3% sodium pentobarbital intramuscular injection. Animals weighing less than 45 kg received 1 mL/kg and those weighing greater than 45 kg received 0.5 mL/kg. The pigs were fixed on the operating table after being anesthetized. The abdominal cavity was opened and the liver and diaphragm were exposed. Using the optical fiber handgrip, the axis was set perpendicular to a target tissue surface distance of 2 mm.

Experimental animals and controls were grouped by liver irradiation dose; the diaphragm was scanned and irradiated vertically and horizontally with 1 cm/s fiber movement speed, reciprocated 1, 5, and 10 times. The two groups were assessed for wound illumination mode, vaporization speed, vaporization depth, and wound bleeding. The damage focal distance was greater than 1 cm. Laser output power was measured immediately before and after irradiation. After 30 min, a 1×1 cm lesion was cut at each laser irradiation site, and fixed in 10% formalin solution within 30 s; 8- μm serial paraffin sections were made within 24 h, and stained with hematoxylin and eosin. Observations were made using an optical digital-slice scanning microscope. The deepest slices showing

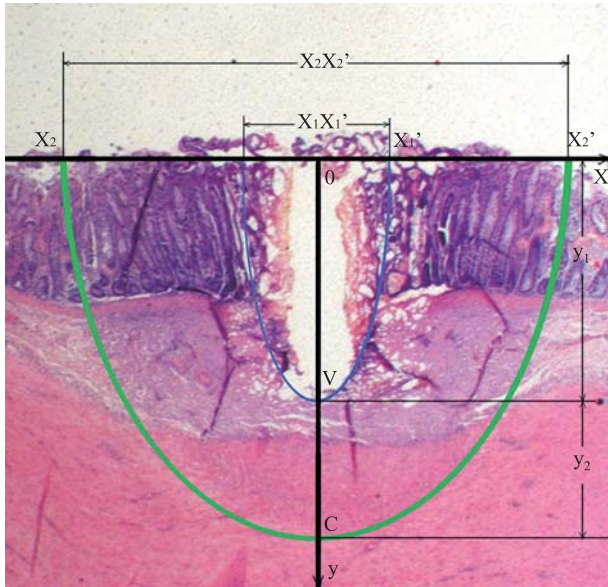


Fig. 2 The microscopic measurement coordinates

laser vaporization in each experimental group were used as the observation object for scanning into digital images stored in the computer. The Medical Image Analysis and Management System was used for true color pathological image evaluation to measure the width of vaporization $X1$ ($X1X1'$), coagulation width $X2$ ($X2X2'$ - $X1X1'$), vaporization depth $y1$ (OV), and coagulation depth $y2$ (VC) (Fig. 2).

The stomach omentum was exposed and an arteriovenous anastomosis was made at the gastroepiploic artery. The arteriovenous diameter was about 2 mm. Using the optical fiber handgrip, the fiber axis was placed along the vertical vessels at a distance of 2 mm. Then, the dual-wavelength laser was used to scan blood vessels measuring 1-2 mm in horizontal diameter; the vessels were cut and observed for hemostasis. Thirty min later, a 1-cm vessel and surrounding tissue were cut from the end of the vessel. Tissue was placed in 10% formaldehyde solution and fixed for 30 s. Longitudinal

sections of blood vessels were made within 24 h; 8- μ m serial paraffin sections were stained with hematoxylin and eosin. Observations were made with an optical microscope for analytical measurement.

Results

When using vertical laser irradiation on the surface of the liver, we observed that superficial tissues retracted to the light point and the color changed from red to white. Tissue vaporized with smoke formation and gradually became pitted. The depressed area was greater than the spot diameter where tissue became charred. Surrounding tissue was dry, hardened, and pale. With tissue evaporation, pits formed in the irradiated area. The depth of penetration gradually increased over time. One control group did not demonstrate tissue depression with vaporization, but demonstrated only local shrinkage and coagulation necrosis. The other two control groups developed pits. However, compared with the area receiving the same dose in the experimental group, there was more sag shallow, more extensive solidification, and thickly charred tissue.

Blood vessels with diameter of 1-2 mm in the experimental and control groups were cut off with no active bleeding.

Liver damage foci were conical and could be divided into vaporization and carbonization zones, a coagulation necrosis layer, and a bleeding congestion and edema layer. Boundaries between the layers were distinct. Using the same parameters, the width and depth of the vaporization zone in the experimental group were greater than those in the control group. Both groups showed a deeply-stained carbonized layer and no fixed shape under the microscope. The experimental group showed charring with a thin but denser texture. The deep layer showed clear coagulation and cell necrosis but the tissue contour was maintained. Liver lobule structure could be seen clearly at low magnification. The experimental group had thinner layer of coagulation necrosis than the

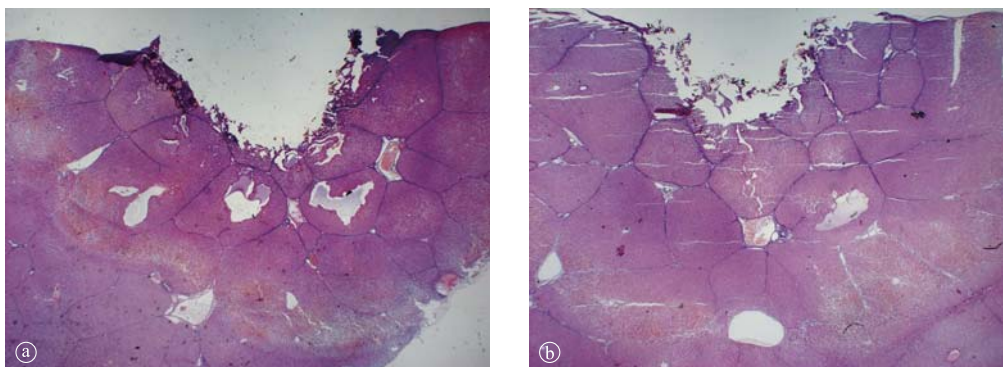


Fig. 3 Experimental results of horizontal scanning irradiation. (a) A 1.32- μ m laser, 50 W, 10 s, horizontal scan, 10 \times 1.25 times; (b) A 1.06- μ m laser, 50 W, 10 s, horizontal scan 10 \times 1.25 times.

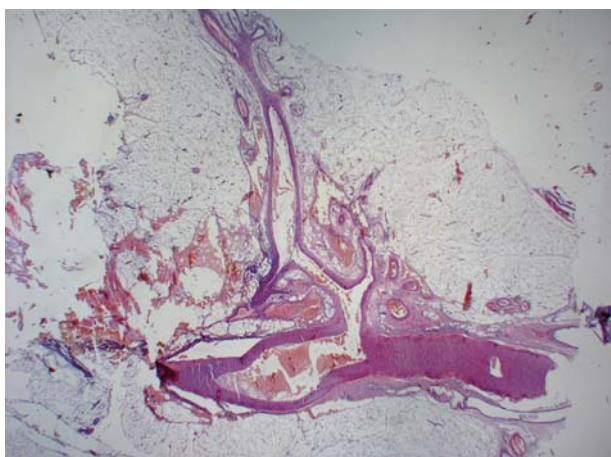


Fig. 4 A 1.32- μ m laser, 50 W, 2-mm vascular longitudinal section, blood vessel thrombosis. 10 \times 1.25 times

control group. The solidified layer showed a bleeding congestion zone, with a large number of red blood cells and thrombosis under the microscope. The outermost layer was edematous, and the transition to normal tissue was undamaged (Fig. 3).

Vascular slices showed sharply cut edges with blood vessels. Outside the cut edge, the vessel wall and surrounding tissue were thick, and had long endovascular thrombosed segments (Fig. 4).

Width and depth of liver tissue vaporization and solidification with vertical irradiation were shown in Table 2. Data from the experimental and control groups were based on the same parameters. $P < 0.01$ was used in the t -test significant differences.

The experimental group showed intravascular thrombus length of 2–4 mm and 2 mm diameter, while the control group showed thrombus length of 2.3–4.9 mm. Thrombosis completely blocked the blood vessels.

Discussion

The liver has large numbers of thick and inflexible peripheral sinuses and a brittle texture, and bleeds easily when damaged. Therefore, liver surgery requires effective hemostasis. We used the liver to determine the efficacy of the 1.32- μ m laser for hemostasis.

The gastroepiploic vessels are relatively thick, with higher pressure and less tissue support. Cutting of blood vessels with scanning laser irradiation mainly relies on intravascular blood becoming heated and solidifying, but does not induce hemostasis by coagulation of thicker layers. The extent of thrombosis depends on the thermal effects produced in the vessels. The control group had a lower water absorption laser coefficient with a significant volume effect. The area of thrombosis in the control group had a greater length than in the experimental group.

Table 2 Comparison of the data of two wavelength vertical irradiation of the liver tissue

| Time (s) | Measurements | Laser wavelength (μ m) | |
|----------|----------------------|-----------------------------|--------------------|
| | | 1.32 | 1.06 |
| 1 | Vaporization width | 863.8 \pm 225.0 | 0.00 |
| | Solidification width | 2047.3 \pm 91.5 | 1561.6 \pm 280.2 |
| | Vaporization width | 362.5 \pm 128.2 | 0.00 |
| | Solidification width | 1647.1 \pm 26.9 | 1216.0 \pm 177.4 |
| 5 | Vaporization width | 1957.8 \pm 531.9 | 1183.5 \pm 310.2 |
| | Solidification width | 2449.7 \pm 151.5 | 4973.3 \pm 297.6 |
| | Vaporization width | 1912.4 \pm 271.3 | 532.3 \pm 223.7 |
| | Solidification width | 1726.1 \pm 88.2 | 3619.5 \pm 206.4 |
| 10 | Vaporization width | 1882.5 \pm 437.1 | 1425.5 \pm 394.0 |
| | Solidification width | 2514.2 \pm 82.6 | 4117.2 \pm 511.1 |
| | Vaporization width | 3316.2 \pm 501.2 | 1388.5 \pm 312.2 |
| | Solidification width | 2874.6 \pm 121.9 | 4463.2 \pm 198.9 |

Both lasers were able to block blood vessels to achieve hemostasis with no bleeding.

Using the same parameters and dose conditions, vaporization width and depth with the 1.32- μ m laser was greater than with the 1.06- μ m laser; therefore, the 1.32- μ m laser had greater vaporization efficacy than the 1.06- μ m laser. Both lasers controlled active bleeding. The solidified layer was about 3 mm thick with the 1.32- μ m laser, but thicker with the 1.06- μ m laser. Coagulation thickness using both lasers met the requirements of hemostasis.

For gastroepiploic vessels less than 2 cm in diameter, both the 1.32- μ m and 1.06- μ m lasers could induce clots within the blood vessels through coagulation to achieve hemostasis.

Conflicts of interest

The authors indicated no potential conflicts of interest.

References

- Alshami MA. Long-pulsed 532-nm Nd:YAG laser treatment for small acquired melanocytic nevi in a single session: an 8-year study on 350 Yemeni patients. *J Cosmet Laser Ther*, 2014, 16: 14–20.
- Bernstein EF, Basilavecchio L, Plugis J. Bilateral axilla hair removal comparing a single wavelength alexandrite laser with combined multiplexed alexandrite and Nd:YAG laser treatment from a single laser platform. *J Drugs Dermatol*, 2012, 11: 185–190.
- Zhang H, Li P, Chen X, *et al*. Raman operation around 1.2 μ m within a diode-pumped actively Q-switched ceramic Nd:YAG/SrWO₄ laser. *Appl Opt*, 2014, 53: 4039–4043.
- Talab SS, McDougal WS, Wu CL, *et al*. Mucosa-sparing, KTP laser coagulation of submucosal telangiectatic vessels in patients with radiation-induced cystitis: a novel approach. *Urology*, 2014, 84: 478–483.
- Kirschbaum A, Braun S, Rexin P, *et al*. Comparison of local tissue damage: monopolar cutter versus Nd: YAG laser for lung parenchyma resection. An experimental study. *Interact Cardiovasc Thorac Surg*,

- 2014, 1: 1–6.
6. Hauser J, Iselin CE. An innovative laser for the minimally invasive treatment of benign prostatic hyperplasia. *Rev Med Suisse*, 2012, 8: 2340–2343.
 7. Bille JF, Niemi MH. *Laser in der Augenheilkunde*. 1993, 24: 109–116.
 8. McKenzie AL. Physics of thermal processes in laser-tissue interaction. *Phys Med Biol*, 1990, 35: 1175–1209.
 9. Wright R, Protsenko DE, Diaz S, *et al*. Shape retention in porcine and rabbit nasal septal cartilage using saline bath immersion and Nd:YAG laser irradiation. *Lasers Surg Med*, 2005, 37: 201–209.
 10. Eichler J, Kim BM. Nonlinear scattering in hard tissue studied with ultrashort laser pulses. *Z Med Phys*, 2002, 12: 191–197.
 11. Fried NM. Therapeutic applications of lasers in urology: an update. *Expert Rev Med Devices*, 2006, 3: 81–94.
 12. Hodgson N, Nighan WL, Golding DJ, *et al*. Efficient 100W Nd:YAG laser operating at a wavelength of 1.44 μm . *Opt Lett*, 1994, 19: 1328–1330.
 13. Zubeev P, Rotkov A, Vaganov I, *et al*. Resection of parenchymatous organs using pulse YAG:Nd laser radiation at 1.44 μm and 1.32 μm wavelengths. *SPIE*, 1999, 3590: 439–445.

DOI 10.1007/s10330-016-0212-2

Cite this article as: Han L, Gao WY, Shen YY, *et al*. Use of 1.32- μm and 1.06- μm wavelength lasers for vascular cutting in a porcine model of liver and stomach bleeding. *Oncol Transl Med*, 2017, 3: 160–164.